



# Bacterial Growth and Death on Cotton Fabrics Conformally Coated with ZnO Thin Films of Varying Thicknesses via Atomic Layer Deposition (ALD)

RENEE U. PUVVADA,<sup>1,2</sup> JAMIE P. WOODING ,<sup>1</sup>  
MICHAEL C. BELLAVIA,<sup>2,3</sup> EMILY K. MCGUINNESS,<sup>1</sup>  
TODD A. SULCHEK,<sup>2,3,4</sup> and MARK D. LOSEGO ,<sup>1,5</sup>

1.—School of Materials Science and Engineering, Georgia Institute of Technology, Atlanta, GA, USA. 2.—The Parker H. Petit Institute for Bioengineering and Bioscience, Georgia Institute of Technology, Atlanta, GA, USA. 3.—Wallace H. Coulter Department of Biomedical Engineering, Georgia Institute of Technology and Emory University, Atlanta, GA, USA. 4.—The George W. Woodruff School of Mechanical Engineering, Georgia Institute of Technology, Atlanta, GA, USA. 5.—e-mail: losego@gatech.edu

Hospital fabrics are commonly exposed to multiple patients and contaminated surfaces between washing/sterilization cycles. Consequently, these textiles act as vectors for the spread of diseases, especially bacterial pathogens. Many modification schemes have been proposed to mitigate the growth and spread of bacteria on fabrics, including use of antimicrobial metal oxide nanoparticles. The aim of this study is to examine the effectiveness of conformal nanoscale ZnO coatings applied to cotton fabrics via atomic layer deposition to control bacterial spread. We find that, at low ZnO loading fractions, bacteria metabolize Zn<sup>2+</sup> ions and reproduce more rapidly. However, as the ZnO loading is increased, the higher concentrations of Zn<sup>2+</sup> overwhelm the bacteria and the nanocoatings become effective antibacterial treatments, killing all bacteria present. These results map out an important design space for implementing ZnO coatings as a potential antimicrobial treatment for textiles and other surfaces.

## INTRODUCTION

Textiles are ubiquitous in modern life. Humans encounter textiles daily in their clothing, linens, and upholstery. In the healthcare industry, this ubiquity can make textiles a dangerous vector for the spread of disease.<sup>1</sup> The contribution of textiles to healthcare-associated infections (HAIs) is a growing concern. According to the Centers for Disease Control and Prevention (CDC), HAIs are defined as infections caused by invasive devices and procedures used on patients during the processes of treatment and recovery;<sup>2</sup> they are a major health and financial issue, as they can increase patient mortality rates, length of hospital/healthcare facility stays, and medical costs.<sup>3,4</sup> While nosocomial

infections are commonly caused by medical devices including catheters and ventilators, healthcare textiles to which patients are exposed during procedures and recovery, such as curtains, white coats, and scrubs, can exhibit pathogenic and bacterial contamination that can be passed between healthcare workers and patients.<sup>1,4–7</sup> As such, there is a growing need in the healthcare industry for antibacterial fabrics to reduce risks associated with cross-contamination and transmission of pathogens.<sup>1,3</sup>

Inorganic metal oxides, including ZnO, MgO, and CaO, have demonstrated antibacterial activity against *Escherichia coli* (*E. coli*) and *Staphylococcus aureus*.<sup>8,9</sup> The antibacterial activity of these metal oxides is believed to be a consequence of their dissolution into metal ions, which can be cytotoxic to bacteria. These metal ions (Zn<sup>2+</sup>, Mg<sup>2+</sup>, and Ca<sup>2+</sup>) are also essential for enzymatic activity and gene

Renee U. Puvvada and Jamie P. Wooding have contributed equally to this work.

expression in many bacteria, but when delivered in excess, they can overwhelm the bacteria, cause growth inhibition, and lead to cell death.<sup>10–13</sup>

Previously, inorganic metal oxides have been incorporated as antibacterial agents in fabrics via sol–gel,<sup>14–16</sup> wet chemical (aqueous),<sup>17,18</sup> spray pyrolysis,<sup>19–21</sup> electrodeposition,<sup>22,23</sup> and hydrothermal methods.<sup>24,25</sup> The aim of this work is to study how bacteria interact with fabrics conformally coated with nanoscale ZnO thin films via atomic layer deposition (ALD). As reported by Hyde et al.,<sup>26,27</sup> and Lee et al.,<sup>28</sup> ALD enables vapor-phase precursors to penetrate and coat complex fiber structures in a conformal and uniform fashion to alter surface properties of the substrate. As such, we leverage the conformality and deposition precision unique to the ALD process to systematically control the thickness of the ZnO coating on cotton fabrics from 0.2 nm to 20 nm and to study the variation in the bacterial response with the extent of ZnO loading. We find that, for low loading levels, it is possible to increase bacterial growth, while higher loading fractions achieve the more desirable, antibacterial effects.

## METHODS

### Materials

Single-fill plain-weave 100% cotton fabrics were purchased from Mybecca, Inc. (Los Angeles, CA, USA), and used as received. Prior to use, material was stored at approximately 24°C and 20% relative humidity. Fabrics were exposed to DH5- $\alpha$  strain of *E. coli*, a strain commonly utilized for laboratory processes to assess the antibacterial response of a substance.

### Atomic Layer Deposition

Woven cotton fabrics were conformally coated with ZnO films using ALD. ALD is a well-established thin-film deposition technique in which vapor phase-precursors are sequentially delivered to a substrate and undergo self-limiting surface reactions, depositing a film “atomic-layer-by-atomic-layer.”<sup>29,30</sup> In this work, ZnO ALD was conducted in a custom-built, hot-walled, flow-tube reactor (4 in. inner diameter) under continuous flow of N<sub>2</sub> carrier gas at 2 Torr and temperature of 90°C. Fabrics were held at 90°C in the 2 Torr flowing nitrogen atmosphere for 10 min prior to deposition to reduce the amount of adsorbed water. Diethylzinc [DEZ, 95% purity, Zn(C<sub>2</sub>H<sub>5</sub>)<sub>2</sub>] from Strem Chemicals (Newburyport, MA, USA) and deionized (DI) water were used as ALD precursors with dosing sequence of 1.0 s DEZ dose/45 s N<sub>2</sub> purge/1.0 s H<sub>2</sub>O dose/60 s N<sub>2</sub> purge, controlled using a custom LabVIEW programming environment.<sup>31</sup> Cotton fabrics were coated with 1–100 cycles of this DEZ/H<sub>2</sub>O sequence, corresponding to approximately 0.2–20 nm of ZnO. The ZnO coating thickness on the

cotton fabrics was estimated based on film thickness measurements performed on Si wafers, present as monitor wafers in the deposition chamber, via spectroscopic ellipsometry (alpha-SE, J.A. Woollam Co., Lincoln, NE, USA) and are consistent with reported growth rates on SiO<sub>2</sub> surfaces at low temperatures.<sup>32,33</sup>

### Chemical and Structural Analysis

Fiber and film microstructure were studied via optical microscopy (Leica DVM6 Digital Microscope, Leica Microsystems, Buffalo Grove, IL, USA) and scanning electron microscopy (SEM; Phenom ProX SEM, Phenom World, Eindhoven, The Netherlands). To study the coating conformality and continuity, 100-cycle ZnO-coated cotton fabrics underwent 650°C heat treatment in air for 4 h to burn out (pyrolyze) the cotton fabrics such that the remaining ZnO structure could be imaged. Energy-dispersive x-ray (EDX) spectroscopy was used to analyze the spatial arrangements of the elemental composition of the treated and untreated fabrics. All EDX measurements were carried out at electron beam accelerating voltage of 15 kV. Thermogravimetric analysis (TGA; PerkinElmer TGA 4000, PerkinElmer, Waltham, MA, USA) was performed to determine the weight percent of ZnO on the cotton fabrics post-ALD treatment. A standard TGA run consisted of holding 5 mg of fabric in a ceramic sample pan at 110°C for 60 min to remove water, then ramping the temperature from 110°C to 900°C at 10°C/min in air. This temperature range is sufficient to completely combust the cotton fabric.<sup>34</sup> At least three replicates of each cotton fabric treatment were analyzed, in addition to a set of replicates of the empty ceramic crucible to correct collected data for buoyancy effects. Inductively coupled plasma optical emission spectroscopy (ICP-OES; Optima 7300DV, PerkinElmer, Waltham, MA, USA) was performed to detect chemical elements present. A 1 cm × 1 cm fabric square was placed in 125  $\mu$ L phosphate-buffered saline (PBS) solution for 20 h, and the solution was sampled to determine the concentration of Zn.

### Bacterial Viability Studies

Bacterial growth on both treated and untreated fabrics was studied in both aqueous and pseudo-dry conditions. Prior to the start of all bacterial studies, fabrics were exposed to ultraviolet (UV) light (60 Hz, 40  $\mu$ W/cm<sup>2</sup>) for 15 min to kill any native bacteria. Because this UV light exposure is for a short period of time, it should not cause significant chemical degradation within the cotton fabric,<sup>35</sup> especially since ZnO coatings have been found to impart UV protection.<sup>36</sup> In the initial study, fabric was exposed to bacteria in aqueous conditions. A 1 cm × 1 cm fabric square was placed in a 115- $\mu$ L aliquot of PBS containing 10  $\mu$ L of 5 × 10<sup>11</sup> bacteria/liter of DH5- $\alpha$  *E. coli*, as determined by OD600. The

fabric was incubated in this solution for 20 h. The bacterial solution was then sampled via pipetting and underwent six tenfold dilutions as appropriate before plating on an agar plate (LB Agar, Fisher BioReagents, Miller, Pittsburgh, PA, USA). This concentration of bacteria corresponds to American Association of Textile Chemists and Colorists (AATCC) TM100 protocol and is the same across all experiments;<sup>37</sup> furthermore, bacteria growth was found to be in the log phase during incubation. After culturing the bacteria for 20 h in an incubator (VWR 1535 Incubator, VWR Scientific, Radnor, PA, USA) at 37°C, colony-forming units (CFUs) were visually counted to quantify the concentration of viable bacteria remaining in solution (Supplementary Fig. S-1).

A second method for bacterial growth was undertaken to better approximate the pseudo-dry conditions typically encountered during fabric use. This method is derived from AATCC TM100 protocol.<sup>37</sup> Again, prior to testing, all fabrics were sterilized with UV light for 15 min. Three 48-mm-diameter circular swatches of fabric were then exposed to 1 mL of 100 bacteria/liter concentration bacterial solution, just enough to completely wet all fibers in the fabric. Exposure times between 5 s and 100,000 s (approximately 1 day) were explored. During exposure, fabrics were kept in a sealable sterile 120-mL plastic container to maintain a constant level of “wetness.” After the designated exposure time, fabrics were

transferred to an empty, sterile 120-mL plastic container with 100 mL PBS solution. The container was then agitated by hand for 1 min to collect any bacteria present. The PBS solution was then sampled, diluted appropriately, plated on agar growth media, and incubated at 37°C for 20 h (Supplementary Fig. S-2). The number of CFUs was then counted and averaged across six experiments.

## RESULTS AND DISCUSSION

Figure 1 summarizes the electron microscopy investigation of the ALD ZnO-coated cotton fabrics. The base cotton fabric has a weave structure with yarn diameter of approximately 150–250  $\mu\text{m}$  and individual fiber diameter ranging from 10  $\mu\text{m}$  to 20  $\mu\text{m}$  (Fig. 1a). Because the organometallic ALD precursor, DEZ, is highly reactive towards water, we expect the precursor to readily react with the six hydroxyl groups per monomer unit of cellulose,<sup>27,38</sup> quickly nucleating and creating a conformal metal oxide coating on the cotton fabric. After 100 cycles, the ZnO coating was easily detectable by EDX (Fig. 1b). To further understand the structure of this coating, we burned out (pyrolyzed) the cotton at 650°C in air. Based on the TGA analysis, these conditions were sufficient to fully remove all the cotton (Supplementary Fig. S-5). Figure 1c presents the results of SEM/EDX analysis of these pyrolyzed

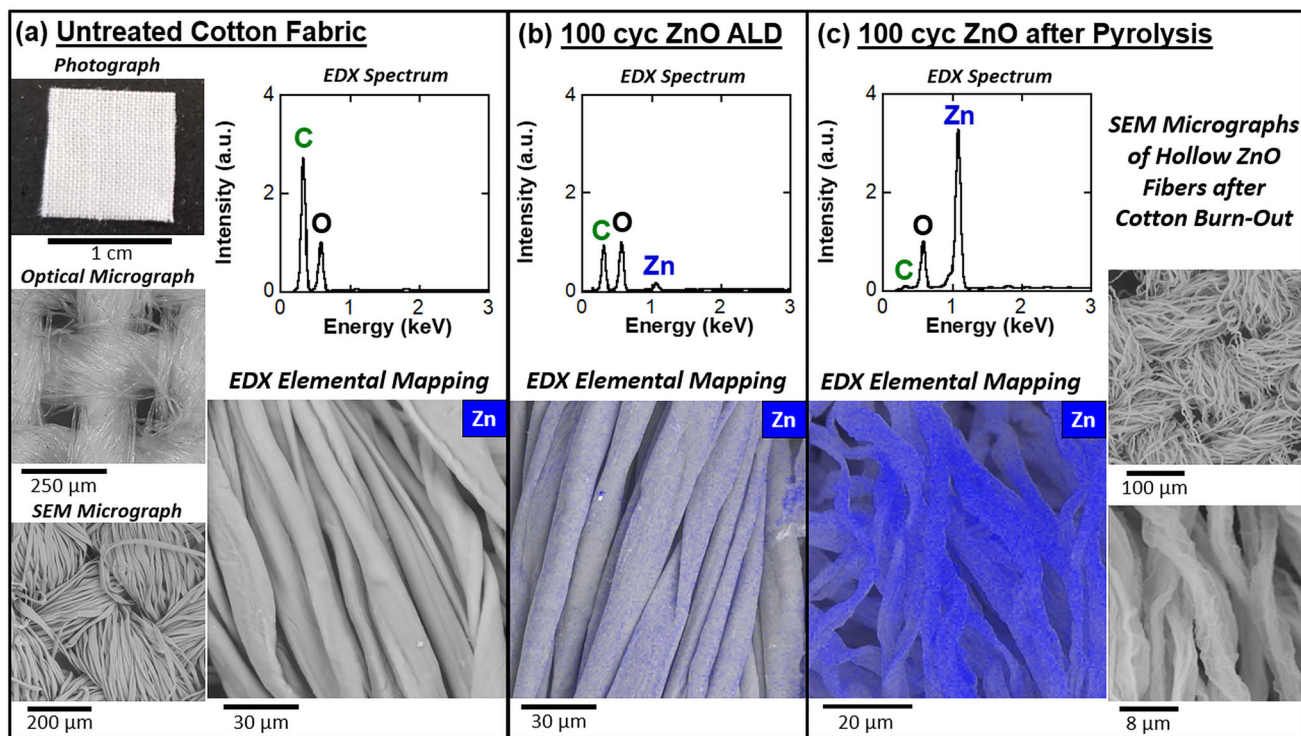


Fig. 1. (a) Photograph, optical micrograph, SEM micrograph, EDX spectrum, and EDX elemental mapping for untreated cotton fabric, (b) EDX spectrum and EDX elemental mapping of 100-cycle ZnO ALD on cotton fabric, and (c) EDX spectrum, EDX elemental mapping, and SEM micrographs of 100-cycle ZnO coating after heat treatment at 650°C for 4 h to remove cotton. All EDX spectra normalized to oxygen peak. All EDX elemental maps display Zn signal only.

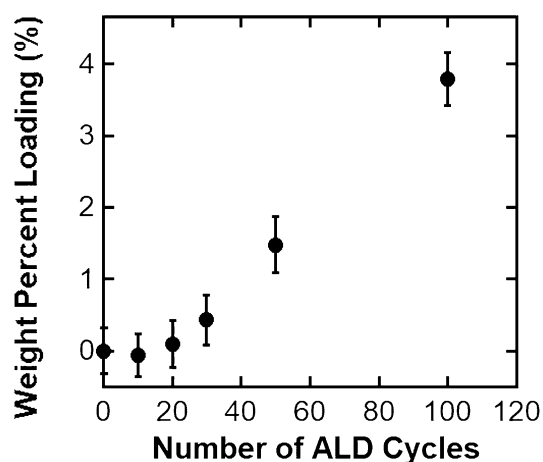


Fig. 2. ZnO mass loading on cotton fabrics as a function of the number of ALD cycles as measured via thermogravimetric analysis (TGA) to 900°C in air.

fabrics, clearly showing hollow tubes of ZnO, which appear “transparent” in SEM, consistent with this ZnO ALD layer originally being conformal to the cotton fibers. In fact, the entire woven structure was maintained, although the yarn diameters shrank to  $\sim 100 \mu\text{m}$  and the fiber diameters to less than  $10 \mu\text{m}$ . EDX spectra showed a marked decrease in carbon signal after pyrolysis, further verifying the removal of cotton, and a marked increase in the Zn signal since the electron beam is now sampling more ZnO fibers and the ZnO fibers have densified. This ability to use ALD to replicate the macro- and microscale structure of cotton fibers is consistent with the previous report by Hojo et al.<sup>39</sup>

To better quantify the ZnO loading on the cotton fabrics, treated fabrics were examined by thermogravimetric analysis. Residual ZnO mass loadings detected via TGA for cotton fabrics coated with 1–100 ALD cycles are summarized in Fig. 2. As expected, the ZnO mass loading increased reasonably linearly with the ALD cycle number. Below 30 ALD cycles, ZnO was undetectable by TGA. Cotton fabrics coated with 100 cycles of ZnO ALD had an average loading of 3.8 wt.% ZnO. This loading dropped to 1.5 wt.% at 50 cycles. Supplementary Table S-I provides complete numerical values for each of these measurements.

We next examined the bacterial growth on fabrics with ZnO films of varying thicknesses fully immersed in aqueous dispersions of *E. coli*. Figure 3 plots the average number of colony-forming units (CFUs) observed for a variety of ZnO film thicknesses as well as for three controls. The error bars in this figure represent the standard error for three trials. Three control conditions were included in this study: (1) bacteria in PBS without fabric (positive control), (2) bacteria in PBS with a swatch of untreated cotton fabric, and (3) bacteria in ethanol (negative control). For the positive control (cells only), we measured 19.7 CFUs of *E. coli* per 115  $\mu\text{L}$  PBS. When cotton fabric was added to the

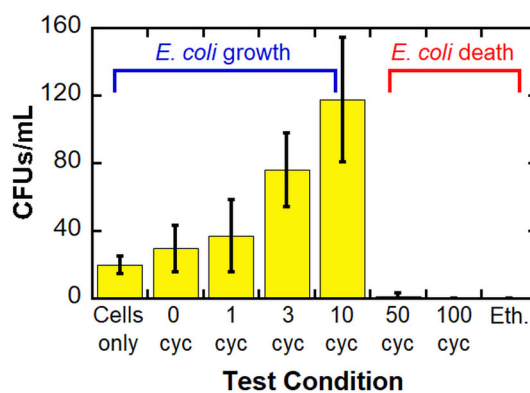


Fig. 3. Concentration of *E. coli* colony-forming units after aqueous exposure to cotton fabrics with ZnO coatings of varying thicknesses. “0 cyc” indicates testing a fabric without coating (untreated), while 1, 3, 10, 50, and 100 cycles are fabrics coated with this number of ZnO ALD cycles. Data for a positive control (cells only) and negative control (ethanol) are also included.

bacterial PBS solution, we observed a 50% increase in the average number of bacteria present. As such, we are in agreement with Selvam et al.<sup>40</sup> in concluding that untreated cotton fabric does not exhibit antibacterial properties. Interestingly, a statistically significant increase in bacterial growth was observed for cotton fabrics coated with 1, 3, and 10 cycles of ZnO ALD. At 10 cycles of ZnO ALD, the bacterial growth increased by more than five times compared with the positive control. In this regime, we propose that ZnO is dissolving and the  $\text{Zn}^{2+}$  ions are acting as a nutrient for bacterial growth.<sup>9,11,13,41,42</sup> In contrast, as the number of cycles was increased to over 50 (coating thickness approximately 10 nm), bacterial growth was significantly suppressed; cotton fabrics coated with 100 cycles of ZnO ALD consistently showed no bacterial growth in PBS solution. At these ZnO loadings, the  $\text{Zn}^{2+}$  ion concentration appears cytotoxic towards *E. coli*.<sup>9,12,42</sup>

While the exact mechanism of the interaction of nano-ZnO with bacterial species is generally not agreed upon,<sup>9,42</sup> Espitia et al.<sup>9</sup> delineate three main reported mechanisms for the antibacterial activity of metal oxides: (1) release of antibacterial ions, (2) interaction of nanoparticles with bacteria, causing damage to the cell membrane, and (3) formation of reactive oxygen species (ROS) from light radiation. To determine whether zinc ions were released into solution as proposed in mechanism 1, ICP-OES was conducted on 12.5 mL PBS solutions that were exposed to cotton fabrics with 100-cycle ZnO ALD. After 20 h of immersion, the concentration of Zn was 0.255 mg/L, while after 96 h of immersion, it was 0.243 mg/L. As such, ZnO does dissolve when the cotton fabric is immersed in saline solution, reaching saturation by 20 h of incubation. Mechanism 2, the interaction of nanoparticles with bacteria, does not appear to be the primary cause of antibacterial activity in this study, because nanoparticles are not present on the cotton fabric

surface to interfere with the cell membrane. With respect to mechanism 3, we cannot fully eliminate this effect because this study did not carefully control for light versus dark exposure conditions. However, only mechanism 1 would cause the enhanced bacterial growth at low ZnO loading fractions as observed in this study, hence we focus on this mechanism.

Prior reports have indicated that zinc, in proper concentrations, is a cofactor for over 300 proteins and functions in bacterial enzymatic activity and transcription.<sup>9–11,43</sup> Bacteria rely on their transport protein systems to regulate  $Zn^{2+}$  uptake and efflux to maintain a critical homeostatic concentration within the cell interior. Figure 4a illustrates the  $Zn^{2+}$  transport protein system for low concentrations of  $Zn^{2+}$  ions, while Fig. 4b illustrates a different transport protein system employed by bacteria at high  $Zn^{2+}$  concentration. As seen in Fig. 4a, low concentrations of zinc ions enhance metabolic activity, thereby contributing to the increased rate of

reproduction seen for *E. coli* exposed to fabrics coated with 1–10 cycles of ZnO (corresponding to approximately 0.2-nm- to 2-nm-thick ZnO nanocoatings). For these ultrathin coatings, the dissolved  $Zn^{2+}$  ions are essentially acting as a nutrient that encourages bacterial growth. However, if the  $Zn^{2+}$  concentration is too high, the bacteria's ion transport pathways are overwhelmed, leading to toxicity by metal intoxication.<sup>10,43</sup> While this precise concentration is unknown, Fig. 3 demonstrates that at least 50 cycles of ZnO ALD supplied a sufficient concentration of  $Zn^{2+}$  to overwhelm the bacteria's transport systems, resulting in cytotoxicity.

To better understand the extent to which ZnO dissolution and cytotoxicity is possible under “less wet” conditions, we conducted a second series of experiments using drier test conditions. In this series of pseudo-dry tests, a stack of three treated cotton swatches, each 4.8 cm in diameter, were dampened with 1 mL bacterial solution for only 5 s, in accordance with AATCC TM100 protocol.<sup>37</sup> After the swatches were dampened, exposing the bacteria to the ALD ZnO coating, they were transferred to a sterile jar with 100 mL sterile PBS then shaken for 1 min to collect the exposed bacteria. This solution was then sampled and plated on agar dishes. The dishes were incubated for 20 h, and the resultant colonies were counted. Figure 5 presents the results of this experiment. The error bars in this figure represent the standard error for six trials. Again, higher bacteria growth was observed for fabrics coated with 10 cycles of ZnO. At 100 ALD cycles, bacterial growth decreased but remained higher than the positive control. We suspect that this continued growth is a result of suppressed ZnO dissolution because (1) the fabric is no longer fully immersed in aqueous solution and (2) the exposure time is only 5 s. As such, comparison of Figs. 3 and 5 demonstrates the significance of fully immersing

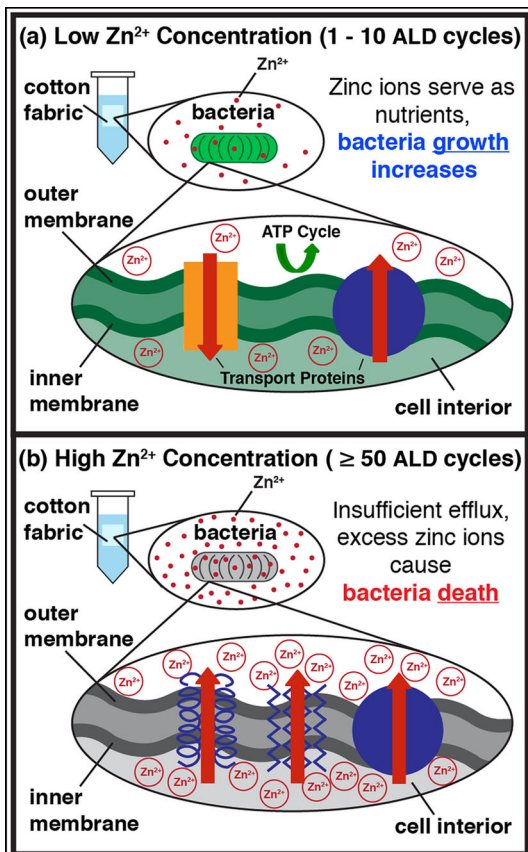


Fig. 4. Schematic of proposed  $Zn^{2+}$  interaction with bacteria observed for ZnO ALD-coated cotton fabrics exposed to aqueous (PBS) solutions of *E. coli*, with (a) low and (b) high concentrations of zinc ions. In each of the panels, the upper left image designates treated cotton fabric in bacterial solution, the upper middle image depicts a magnified schematic of bacteria in solution with zinc ions (red circles), and the lower middle image is a further magnified schematic of the bacterial membrane and its transport proteins interfacing with zinc ions. Adapted from Ref. 41 (Color figure online).

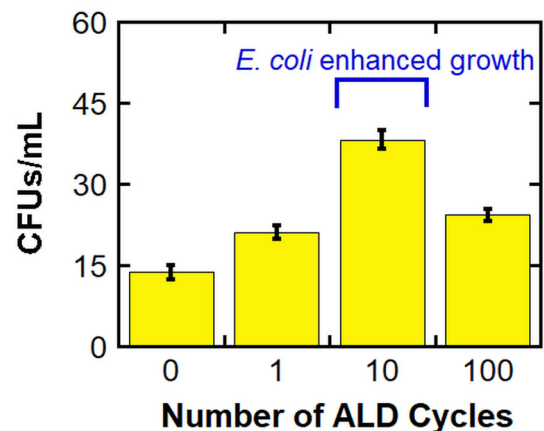


Fig. 5. Concentration of *E. coli* colony-forming units for cotton fabrics subjected to varying numbers of ZnO ALD cycles tested via exposure to small volumes of PBS bacterial solution (pseudo-dry conditions) for 5 s. These tests were based on the AATCC TM100 standard.<sup>37</sup>

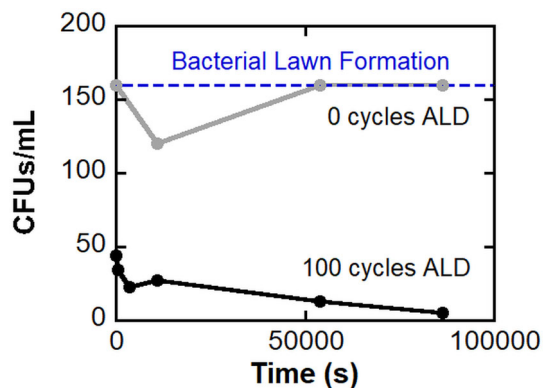


Fig. 6. Concentration of *E. coli* colony-forming units for untreated cotton and cotton with 100 cycles of ZnO ALD tested via exposure to small volumes of PBS bacterial solution (pseudo-dry conditions) for varying times. The dotted line at 160 CFUs/mL represents bacterial lawn formation (uncountable).

the cotton in aqueous solution and allowing longer exposure times in solution to enable dissolution and ion release to create a more pronounced bacterial response.

We conducted a temporal exposure study under these pseudo-dry conditions to determine the effects of dissolution kinetics on cytotoxicity. In this third experiment, untreated cotton fabric and fabric coated with 100 cycles of ZnO ALD were exposed to the bacterial solution for varying amounts of time up to 1 day. Figure 6 plots the number of colony-forming units (CFUs) counted as a function of exposure time. The 100-cycle ZnO-coated cotton fabric consistently showed fewer CFUs than the untreated fabric. In fact, the untreated fabric even demonstrated growth of bacterial lawns for three of the four collected data points, in which the agar plate was completely saturated with bacteria growth; these garner an assigned value of 160 CFUs for the minimum number of colonies fitting in the plate area.<sup>44</sup> In contrast, the ZnO-coated fabric demonstrated a clear decreasing trend in the number of CFUs with exposure time. After 1 day, nearly all the bacteria were killed. Therefore, greater exposure time resulted in significantly fewer colony-forming units on the ZnO-coated fabric, reinforcing the proposed condition that sufficient  $Zn^{2+}$ , as determined by the amount deposited and the exposure time, must enter the bacteria for the cotton fabric to exhibit antibacterial properties.

## CONCLUSION

Atomic layer deposition (ALD) was used to study the interactions of *E. coli* bacteria with ZnO nanocoatings with systematically varying thickness (0.2–20 nm) on cotton fabrics. Both aqueous and pseudo-dry test conditions were evaluated. While Kääriäinen et al.<sup>45</sup> previously demonstrated that “thick” ( $\geq 45$  nm) ALD ZnO films grown on glass are antibacterial, this study demonstrates that the ZnO–bacteria interaction is film thickness dependent. In

fully aqueous conditions, monotonic increase in bacteria growth was observed for cotton fabrics coated with up to 10 cycles of ZnO ALD ( $\sim 2$  nm). At 50 cycles ( $\sim 10$  nm) and beyond, complete bacterial death was observed. Here, we propose that the mechanism for this interaction is dissolution of  $Zn^{2+}$  ions. At low  $Zn^{2+}$  concentrations, the ion acts as a nutrient, whereas at higher loadings it becomes cytotoxic towards *E. coli*. Similar enhanced growth was observed for up to 10 ZnO ALD cycles in pseudo-dry growth conditions. However, for these pseudo-dry conditions, cytotoxicity required substantial time to occur, as 100-cycle ZnO ALD coatings ( $\sim 20$  nm) required approximately 1 day to cause complete *E. coli* death. As such, the antibacterial efficacy is dependent upon concentration and time, as is the solubility of metal oxides. These results indicate the importance of both the ZnO loading fraction and environmental test conditions for the efficacy of ZnO as an antibacterial treatment for fabrics.

## ACKNOWLEDGEMENTS

Funding for this project came from the Georgia Tech President’s Undergraduate Research Award (PURA), the Petit Bioengineering Undergraduate Research Fellowship, and the Roxanne D. Westendorf Undergraduate Research Fund. Additionally, this material is based upon work supported by the National Science Foundation Graduate Research Fellowship Program under Grant No. DGE-1650044. Any opinions, findings, and conclusions or recommendations expressed in this material are those of the authors and do not necessarily reflect the views of the National Science Foundation. Part of this research was conducted in Georgia Tech’s Materials Innovation & Learning Laboratory (The MILL), an uncommon “make and measure” space committed to elevating undergraduate research in materials science. This work was also performed in part at the Georgia Tech Institute for Electronics and Nanotechnology, a member of the National Nanotechnology Coordinated Infrastructure, which is supported by the National Science Foundation (Grant No. ECCS-1542174). Finally, the authors thank Brandon D. Piercy for performing x-ray diffraction for this study.

## CONFLICT OF INTEREST

The authors declare that they have no conflict of interest.

## ELECTRONIC SUPPLEMENTARY MATERIAL

The online version of this article (<https://doi.org/10.1007/s11837-018-3154-z>) contains supplementary material, which is available to authorized users.

## REFERENCES

1. A. Mitchell, M. Spencer, and C. Edmiston Jr., *J. Hosp. Infect.* 90, 285 (2015).
2. Centers for Disease Control and Prevention, *Types of Healthcare-Associated Infections* (Centers for Disease Control and Prevention, 2014, March 26). <https://www.cdc.gov/hai/infectiontypes.html>. Accessed 15 June 2018.
3. I. Perelshtein, A. Lipovsky, N. Perkas, T. Tzanov, M. Arguirova, M. Leseva, and A. Gedanken, *Ultrason. Sonochem.* 25, 82 (2015).
4. K.N. Kelly and J.R. Monson, *Surg. (Oxf.)* 30, 640 (2012).
5. L.S. Munoz-Price, K.L. Arheart, J.P. Mills, T. Cleary, D. DePascale, A. Jimenez, Y. Fajardo-Aquino, G. Coro, D.J. Birnbach, and D.A. Lubarsky, *Am. J. Infect. Control* 40, 245 (2012).
6. J.M. Nordstrom, K.A. Reynolds, and C.P. Gerba, *Am. J. Infect. Control* 40, 539 (2012).
7. G. Suleyman, G. Alangaden, and A.C. Bardossy, *Curr. Infect. Dis. Rep.* 20, 1 (2018).
8. J. Sawai, *J. Microbiol. Methods* 54, 177 (2003).
9. P.J.P. Espitia, N.F.F. Soares, J.S.R. Coimbra, N.J. de Andrade, R.S. Cruz, and E.A.A. Medeiros, *Food Bioprocess Technol.* 5, 1447 (2012).
10. P. Chandrangsu, C. Rensing, and J.D. Helmann, *Nat. Rev. Microbiol.* 15, 338 (2017).
11. A.A. Navarrete, E.V. Mellis, A. Escalas, L.N. Lemos, J.L. Junior, J.A. Quaggio, J. Zhou, and S.M. Tsai, *Agric. Ecosyst. Environ.* 236, 187 (2017).
12. M. Li, L. Zhu, and D. Lin, *Environ. Sci. Technol.* 45, 1977 (2011).
13. K.M. Reddy, K. Feris, J. Bell, D.G. Wingett, C. Hanley, and A. Punnoose, *Appl. Phys. Lett.* 90, 213902 (2007).
14. W.A. Daoud and J.H. Xin, *J. Am. Ceram. Soc.* 87, 953 (2004).
15. H. Zhang and G. Chen, *Environ. Sci. Technol.* 43, 2905 (2009).
16. B. Mahltig, H. Haufe, and H. Böttcher, *J. Mater. Chem.* 15, 4385 (2005).
17. A. Yadav, V. Prasad, A.A. Kathe, S. Raj, D. Yadav, C. Sundaramoorthy, and N. Vigneshwaran, *Bull. Mater. Sci.* 29, 641 (2006).
18. B.A. Holt, S.A. Gregory, T. Sulchek, S. Yee, and M.D. Losego, *A.C.S. Appl. Mater. Interfaces* 10, 7709 (2018).
19. M. Vasanthi, K. Ravichandran, N.J. Begum, G. Muruganantham, S. Snega, A. Panneerselvam, and P. Kavitha, *Superlattices Microstruct.* 55, 180 (2013).
20. A. Arunachalam, S. Dhanapandian, C. Manoharan, and G. Sivakumar, *Spectrochim. Acta Part A* 138, 105 (2015).
21. A.G. Cuevas, K. Balangcod, T. Balangcod, and A. Jasmin, *Procedia Eng.* 68, 537 (2013).
22. Y.Y. Xi, B.Q. Huang, A.B. Djurišić, C.M. Chan, F.C. Leung, W.K. Chan, and D.T. Au, *Thin Solid Films* 517, 6527 (2009).
23. G.J. Chi, S.W. Yao, J. Fan, W.G. Zhang, and H.Z. Wang, *Surf. Coat. Technol.* 157, 162 (2002).
24. N.A. Aal, F. Al-Hazmi, A.A. Al-Ghamdi, A.A. Al-Ghamdi, F. El-Tantawy, and F. Yakuphanoglu, *Spectrochim. Acta Part A* 135, 871 (2015).
25. K.H. Tam, A.B. Djurišić, C.M.N. Chan, Y.Y. Xi, C.W. Tse, Y.H. Leung, W.K. Chan, F.C.C. Leung, and D.W.T. Au, *Thin Solid Films* 516, 6167 (2008).
26. G.K. Hyde, K.J. Park, S.M. Stewart, J.P. Hinestroza, and G.N. Parsons, *Langmuir* 23, 9844 (2007).
27. G.K. Hyde, G. Scarel, J.C. Spagnola, Q. Peng, K. Lee, B. Gong, K.G. Roberts, K.M. Roth, C.A. Hanson, C.K. Devine, and S.M. Stewart, *Langmuir* 26, 2550 (2010).
28. K. Lee, J.S. Jur, D.H. Kim, and G.N. Parsons, *J. Vac. Sci. Technol. A* 30, 01A163 (2012).
29. S.M. George, *Chem. Rev.* 110, 111 (2010).
30. R.L. Puurunen, *J. Appl. Phys.* 97, 9 (2005).
31. B.D. Piercy and M.D. Losego, *J. Vac. Sci. Technol. B* 33, 043201 (2015).
32. E. Guziewicz, I.A. Kowalik, M. Godlewski, K. Kopalko, V. Osinniy, A. Wójcik, S. Yatsunencko, E. Łusakowska, W. Paszkowicz, and M. Guziewicz, *J. Appl. Phys.* 103, 033515 (2008).
33. S.K. Kim, C.S. Hwang, S.-H.K. Park, and S.J. Yun, *Thin Solid Films* 478, 103 (2005).
34. D. Price, A. Horrocks, M. Akalin, and A. Farooq, *J. Anal. Appl. Pyrolysis* 40, 511 (1997).
35. M. Yatagai and S.H. Zeronian, *Cellulose* 1, 205 (1994).
36. A.E. Shafei and A. Abou-Okeil, *Carbohydr. Polym.* 83, 920 (2011).
37. AATCC, *TM100:2004 Assessment of Antibacterial Finishes on Textile Materials*, Developed from American Association of Textile Chemists and Colorists (2004).
38. J. Jur, W.J. Sweet, C.J. Oldham, and G.N. Parsons, *Adv. Funct. Mater.* 21, 1993 (2011).
39. D. Hojo, G. K. Hyde, J. Spagnola, and G. N. Parsons, *MRS Online Proceedings Library*, 1054 (2007).
40. S. Selvam, R. Rajiv Gandhi, J. Suresh, S. Gowri, S. Ravikumar, and M. Sundrarajan, *Int. J. Pharm.* 434, 366 (2012).
41. K. Hantke, *Zinc Biochemistry, Physiology, and Homeostasis* (Dordrecht: Springer, 2001), pp. 53–63.
42. N. Padmavathy and R. Vijayaraghavan, *Sci. Technol. Adv. Mater.* 9, 035004 (2008).
43. M.G. Palmgren, S. Clemens, L.E. Williams, U. Krämer, S. Borg, J.K. Schjørring, and D. Sanders, *Trends Plant Sci.* 13, 464 (2008).
44. B.A. Holt, M.C. Bellavia, D. Potter, D. White, S.R. Stowell, and T. Sulchek, *Biomater. Sci.* 5, 463 (2017).
45. M.L. Kääriäinen, C.K. Weiss, S. Ritz, S. Pütz, D.C. Cameron, V. Mailänder, and K. Landfester, *Appl. Surf. Sci.* 287, 375 (2013).